SUPPLEMENTARY INFORMATION

Rational design of microfluidic templated HA-LPEI nanogels for the targeted delivery of doxorubicin

Emanuele Limiti[a,b†], Eleonora D'Alessandro[a†], Alessio Bucciarelli[c], Sofia Raniolo[a], Pamela Mozetic[b,d,e], Elisa De Luca[b,e], Enrico Domenico Lemma[a,b], Francesco Basoli[a], Giuseppe Gigli[b,f], Fabio Pizzetti[g], Emanuele Mauri[g], Filippo Rossi[g], Marcella Trombetta[a], Sara Maria Giannitelli[a]*, Alberto Rainer[a,b,h]**

[a] Department of Engineering, Università Campus Bio-Medico di Roma, via Álvaro del Portillo 21, 00128 Rome, Italy
[b] Institute of Nanotechnology (NANOTEC), National Research Council, via Monteroni, 73100 Lecce, Italy
[c] BIOtech Research Center and European Institute of Excellence on Tissue Engineering and Regenerative Medicine, Department of Industrial Engineering, University of Trento, Via Delle Regole 101, Trento 38123, Italy
[d] Department of Life Science, Health, and Health Professions, Link Campus University, Rome, Italy
[e] Tecnomed Puglia - Tecnopolo per la medicina di precisione (Biotech Lecce Hub) c/o Campus Ecotekne, via Monteroni, Lecce, 73100 Italy
[f] Department of Experimental Medicine, Università del Salento, via Monteroni, 73100 Lecce, Italy
[g] Department of Chemistry, Materials and Chemical Engineering "G. Natta", Politecnico di Milano, via L. Mancinelli 7, 20131 Milan, Italy
[h] Fondazione Policlinico Universitario Campus Bio-Medico di Roma, via Álvaro del Portillo 200, 00128 Rome, Italy.

Synthesis of Rhodamine azide (RhB-N_3)

Azido terminated-Rhodamine B was synthesized by the following method[46]: 4-azidobutanol spacer was obtained by dissolving 4-chloro-1-butanol (1.5 mL, 15 mmol) in 20 mL of dimethylformamide (DMF) and adding sodium azide (1.17 mg, 18 mmol) at room temperature (RT). The reaction mixture was refluxed at 90 °C for 12 h. Vacuum filtration was used to remove insoluble by-products, and the solution was concentrated under reduced pressure. Residue was re-dissolved in 100 mL of dichloromethane (DCM) and washed with distilled water (DIW) (3 x 100 mL). To remove excess water, the organic phase was dried over magnesium sulfate and filtered using filter paper. Then, the solution was allowed to evaporate at RT to collect the final compound.

Later, the synthesized 4-azidobutanol was reacted with Rhodamine B to obtain RhB-N_3. Briefly: 4-azidobutanol (200 mg, 1.73 mmol) and rhodamine B (504 mg, 1.05 mmol) were dissolved in 20 mL of DCM. Successively, 1-ethyl-3-(3-dimethylaminopropyl) carbodiimide hydrochloride (EDC, 241.5 mg, 1.26 mmol) and 4-(dimethylamino) pyridine (DMAP, 154 mg, 1.26 mmol) were added to the mixture, which was allowed to stir for 24 h at RT. Additionally, consecutive washes with 1 M HCl (3 x 10 mL), 1 M $NaHCO_3$ (3 x 10 mL), and supersaturated NaCl (3 x 10 mL) solutions were

performed. The resulting organic phase was dried over anhydrous sodium sulfate and concentrated under vacuum. Residue was dissolved in tetrahydrofuran (THF) (5 mL), then RhB-N_3 was precipitated by adding diethyl ether (20 mL), collected by vacuum filtration, and dried under reduced pressure. At the end, the final sample was stored at +4 °C until use.

DOX standard calibration curve

A calibration solution of DOX in PBS was prepared by a two-fold dilution (down to 0.02 μM) starting from a DOX concentration of 5 μM. Fluorescence measurements (λex = 488 nm; λem = 590 nm) were recorded on a TECAN M200 spectrophotometer. A standard calibration curve was obtained by plotting fluorescence levels against drug concentration. The linear fitting of the experimental data demonstrated an excellent fit, with an R^2 value of 0.999.

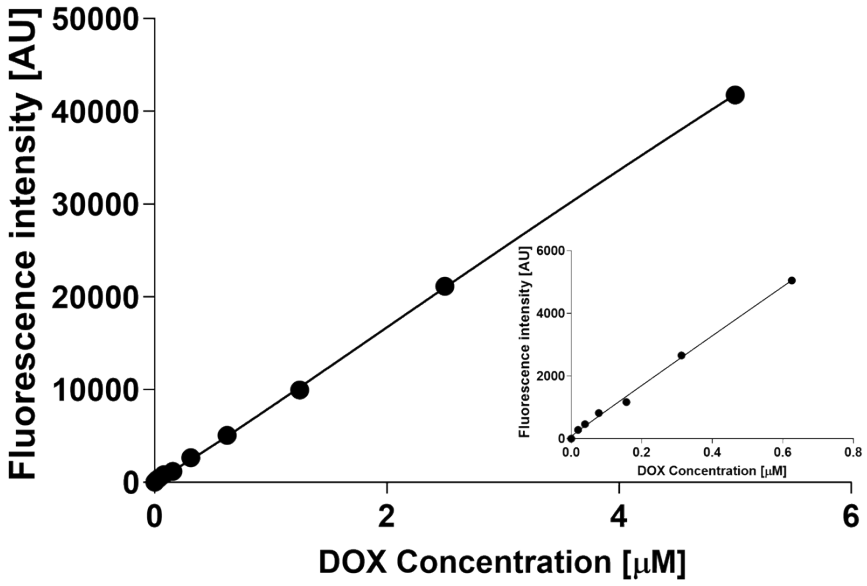

Figure S1 DOX standard calibration curve.

Dose-Response curve of DOX

Figure S2 showed the dose-response curve of DOX evaluated at 24 h on OVCA433 cultured in adhesion using the MTT assay. The value of 4.98 μM was identified as the IC_{50} level. The sublethal concentration of 1 μM used in our work is shown by the black dashed line.

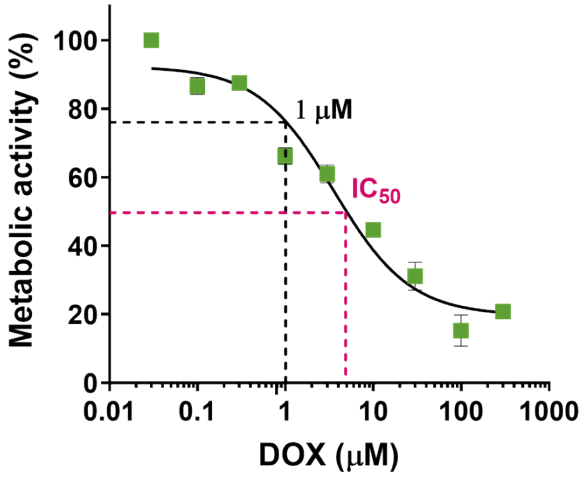

Figure S2 DOX Dose-Response curve. IC_{50} level (purple dashed line) and the used sublethal DOX concentration of 1 μM (black dashed line) are highlighted.

^{1}H-NMR spectra

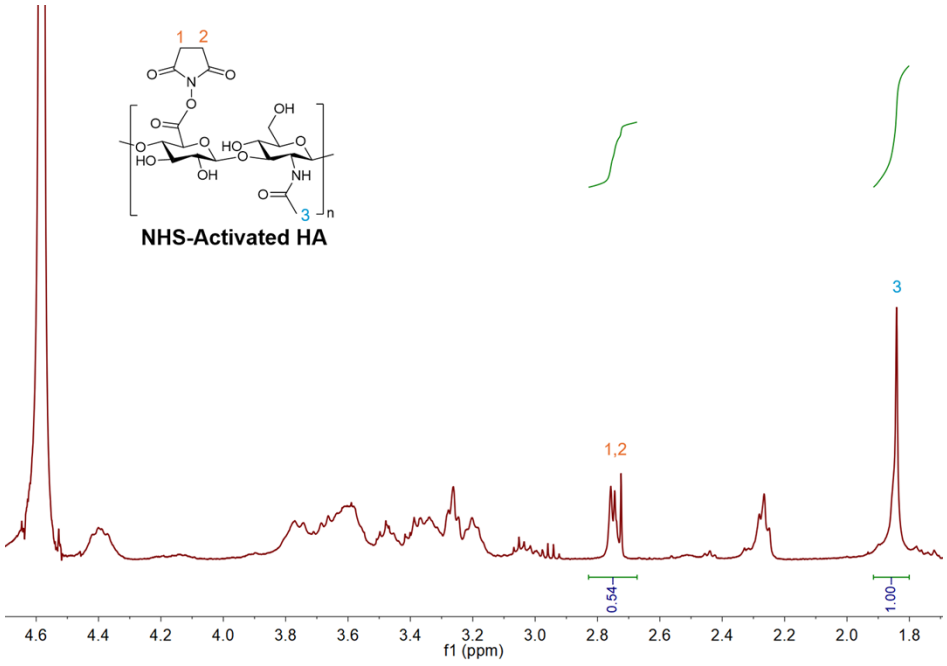

Figure S3 ^{1}H-NMR spectrum of NHS-Activated HA.

The degree of functionalization (DoF) was determined by calculating the ratio of the succinimide signal at 2.75 ppm to the acetyl methyl protons of hyaluronic acid at 1.84 ppm, yielding an estimated DoF of approximately 40.5%.

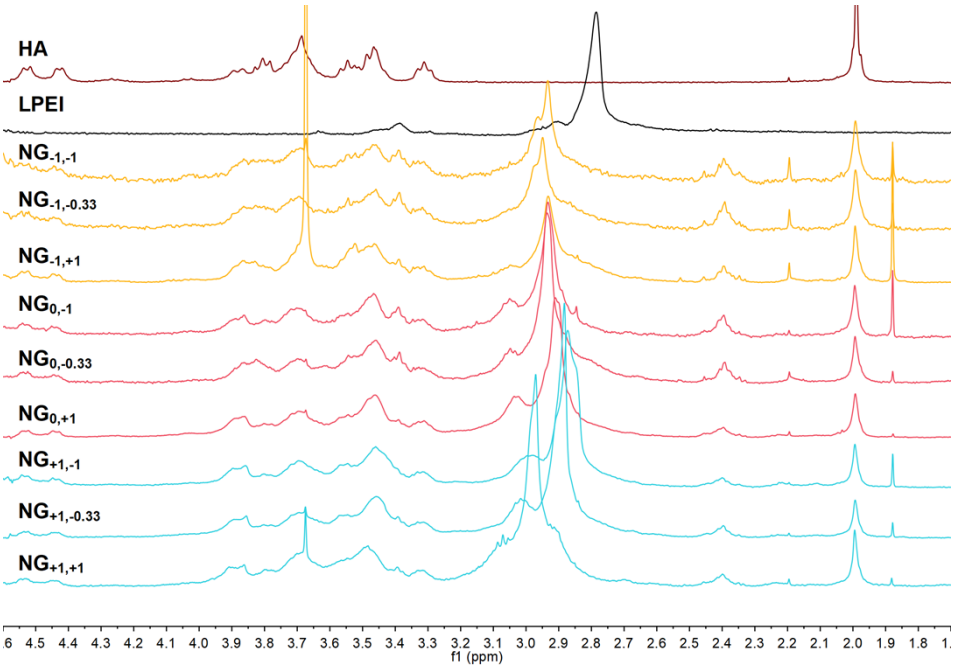

Figure S4 ^{1}H-NMR spectra of each tested synthesis condition. Yellow, red and blue spectra are referred to the NGs synthesized with MR of 5.75, 11.5 and 17.25, respectively.

FTIR spectra

Fourier Transform Infrared Spectroscopic (FTIR) analysis was performed using an Agilent CARY 630 FTIR spectrophotometer (Agilent Technologies, USA), equipped with the MicroLab Expert FTIR software. The spectra were recorded in air at room temperature using a diamond ATR cell with a resolution of 4 cm^{-1}.

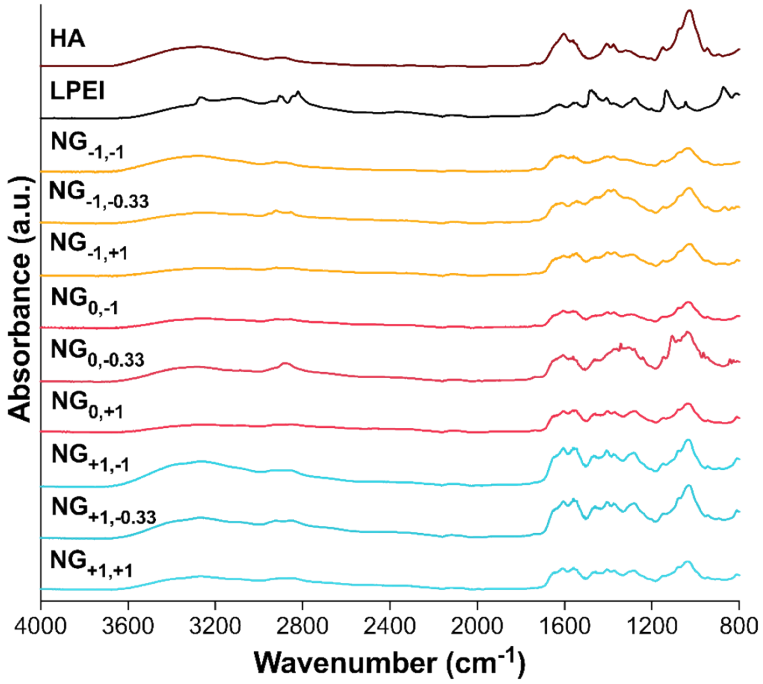

Figure S5 FTIR spectra of each tested synthesis condition. Yellow, red and blue spectra are referred to the NGs synthesized with MR of 5.75, 11.5 and 17.25, respectively.

TEM

Transmission Electron Microscopy (TEM) analysis was conducted using a FEI Tecnai G2 Microscope (Thermo Fisher Scientific). A suspension of NGs were dropped on a lacey carbon coated 300 mesh copper grid (Agar Scientific, Stansted, UK). Samples were dried at 50 °C and TEM images were collected at an acceleration voltage of 120 kV.

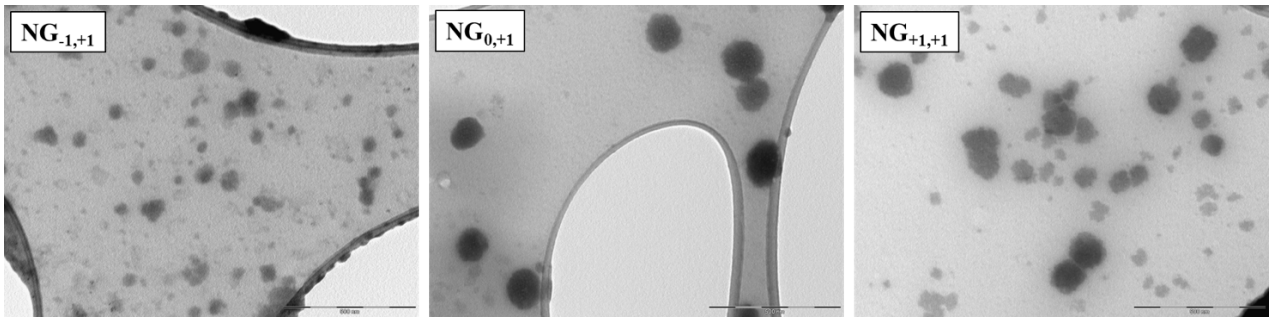

Figure S6 Representative TEM micrographs of three different synthesis condition. Micrographs are referred to the NGs synthesized with FRR = 0.4 and MR 5.75, 11.5 and 17.25, respectively.

ζ - potential

The ζ-potential of NGs were measured using Zetasizer Nano ZS (Malvern Panalytical). In particular, NGs were suspended in ultrapure water (1 mg/mL) and sonicated for 10 min to ensure minimal aggregation of the colloidal system. Readings were performed in triplicate.

Table S1 ζ-potential of the synthesized NGs.

Sample	ζ - potential [mV]
$NG_{-1,-1}$	-14.2 ± 0.7
$NG_{-1,-0.33}$	-17.3 ± 0.9
$NG_{-1,+1}$	1.8 ± 0.2
$NG_{0,-1}$	9.4 ± 0.1
$NG_{0,-0.33}$	12.3 ± 0.6
$NG_{0,+1}$	15.8 ± 0.4
$NG_{+1,-1}$	13.5. ± 1.0
$NG_{+1,-0.33}$	12.2 ± 0.3
$NG_{+1,+1}$	21.1 ± 0.4

Drug release

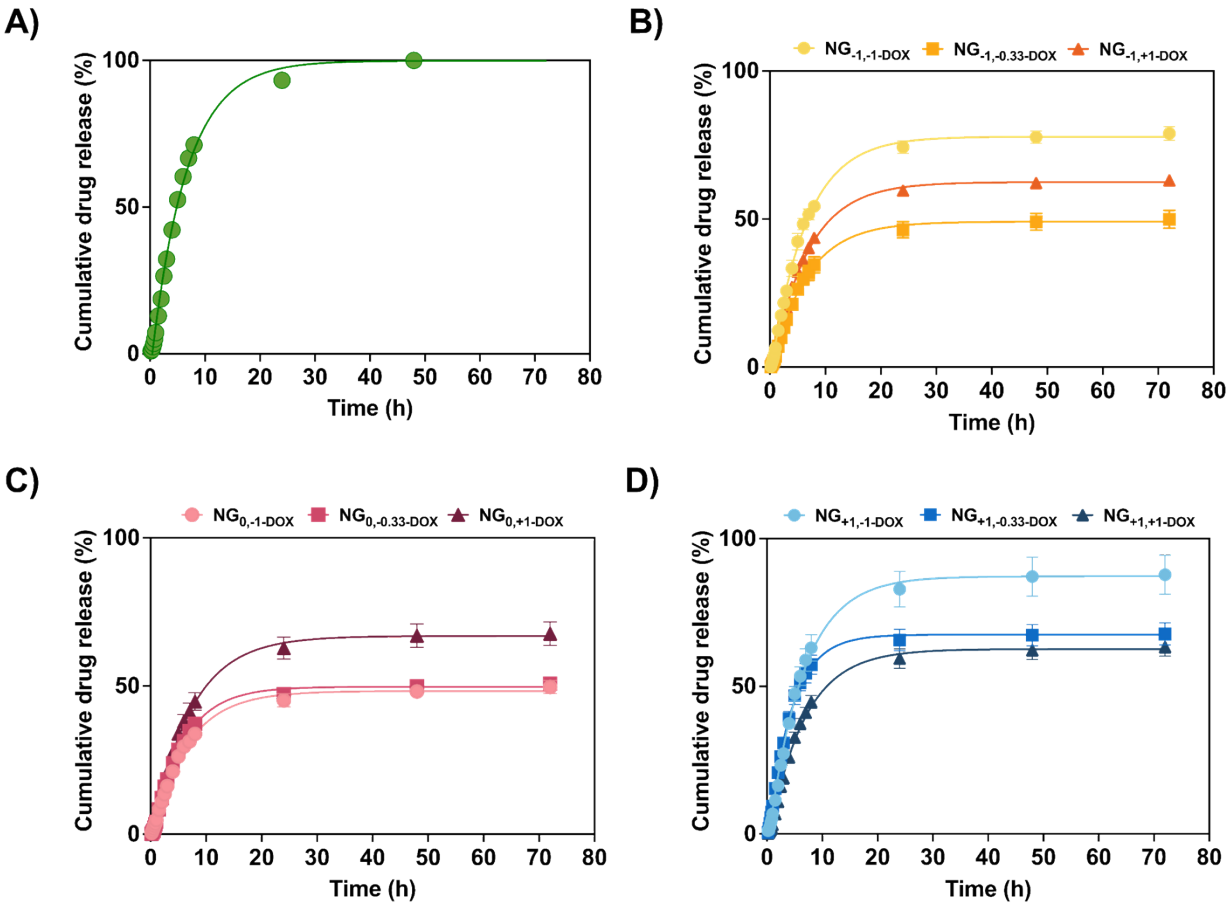

Figure S7 A) Free DOX cumulative release (%). B-D) Drug release curves for NGs synthesized with MR levels of 5.75 (B), 11.5 (C) and 17.25 (D).

From *Figure S6 A* it is possible to appreciate the slow diffusion of DOX through the dialysis bag. The complete release (100%) was achieved only after 48 hours, indicating that the drug-membrane interactions cannot be considered negligible. This same profile can be observed in the release experiments of the DOX-NGs. However, even if the release kinetics has been hindered by the employed experimental setup, the different plateau levels account for a different behavior between the specimens that can be observed.

G6PD assay

NGs cytotoxicity was evaluated through G6PD assay. NGs were administered to the OVCA433 cell line following the protocol described in the manuscript. None of the tested formulations showed altered cell viability after 24h, as reported in *Figure S7*.

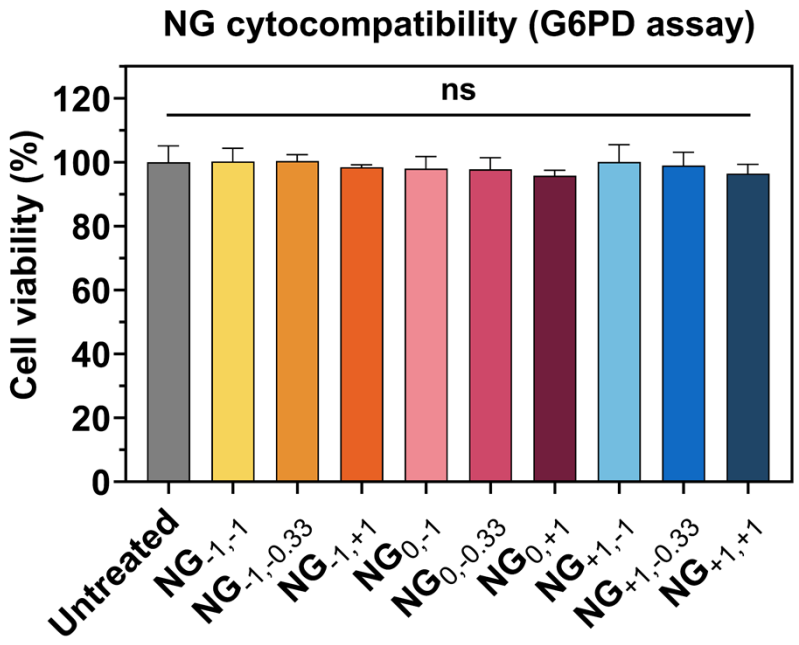

Figure S8 NG cytocompatibility assessed via G6PD assay.

MTT assay

NGs influence on metabolic activity was evaluated through MTT assay. NGs were administered to the OVCA433 cell line following the protocol described in the manuscript.

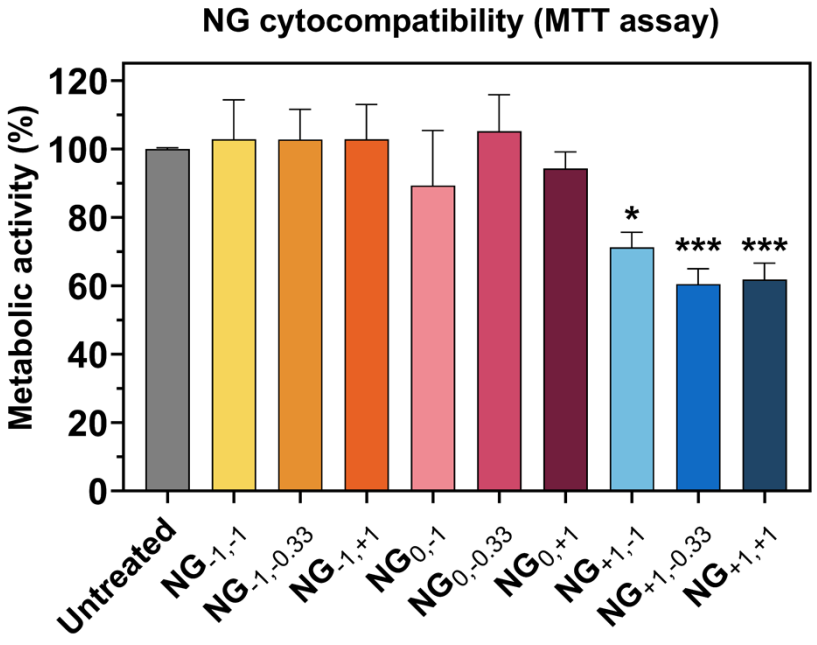

Figure S9 NG cytocompatibility assessed via MTT assay.

Confocal microscopy

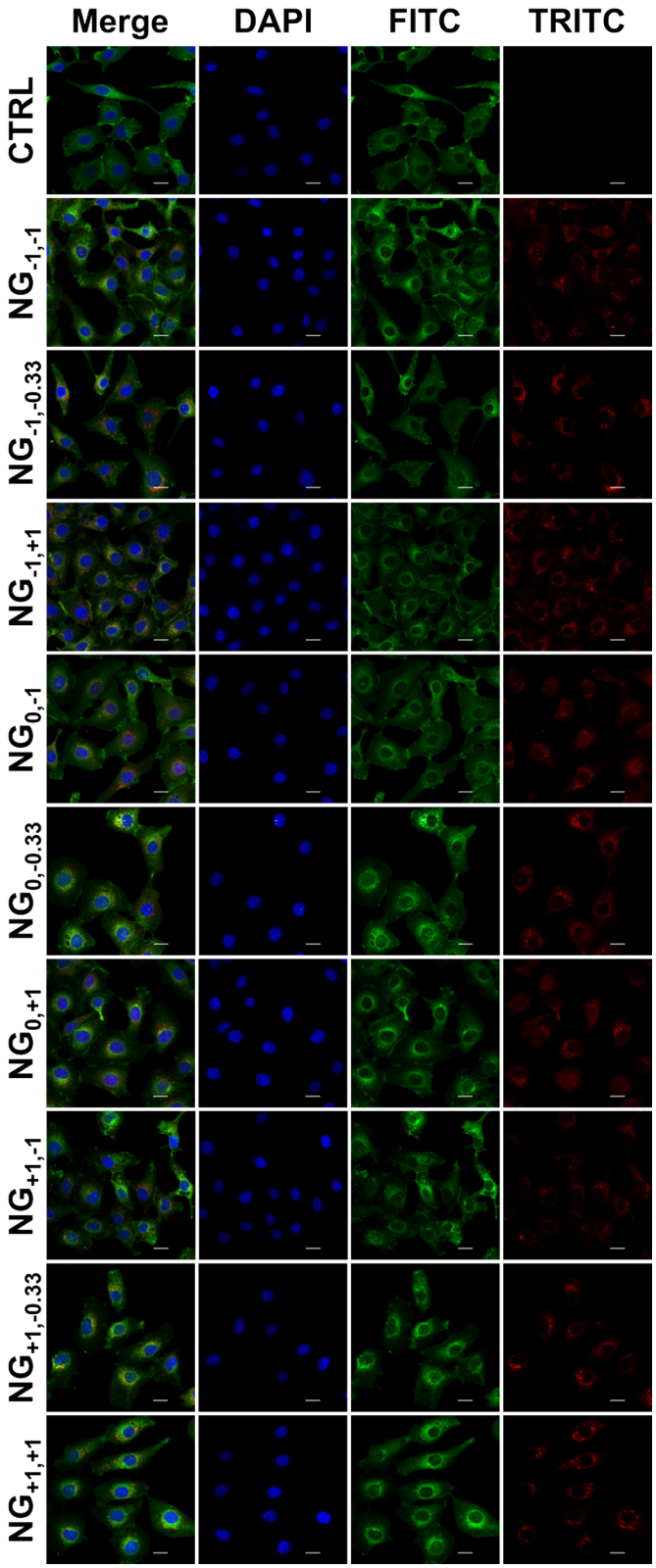

Figure S10 representative fluorescence confocal micrographs. Nuclei are stained with DAPI, cellular membrane with CellMask Green, and red signals are ascribable to the successful NGs internalization. Scale bar 20 μm.

Calculation of corrective factors for flow cytometry

As a first step, the molar ratio $\frac{n_{LPEI}}{n_{HA}}$ between the repeating units of LPEI and HA has been calculated integrating the respective signals of LPEI and HA in each NG spectrum: from 3.417-3.376 ppm and 3.142-2.587 ppm for LPEI, and 4.59-3.419 ppm and 3.336-3.262 ppm for HA.

Successively, we calculated the LPEI/HA weight ratio $\frac{m_{LPEI}}{m_{HA}}$ by taking into consideration the molecular weight (MW) of their respective repeating units:

$$\frac{m_{LPEI}}{m_{HA}} = \frac{n_{LPEI} \cdot MW_{LPEI}}{n_{HA} \cdot MW_{HA}}$$

As the fluorescent dye is linked to LPEI, the corrective factor (CF) must take into account the different amount of LPEI present in each NGs. Thus, we define the LPEI weight fraction as follows:

$$\frac{m_{LPEI}}{m_{NG}} = \frac{m_{LPEI}}{m_{LPEI} + m_{HA}} = \frac{m_{LPEI}/m_{HA}}{m_{LPEI}/m_{HA} + 1}$$

Given the weight fraction of LPEI in each NG formulation, the corresponding corrective factor was defined as:

$$CF_i = \left(\frac{m_{LPEI}}{m_{NG}}\right)_i^{-1}$$

CFs were further normalized to the lowest value:

$$\bar{CF}_i = \frac{CF_i}{min\{CF\}}$$

Empirical model

Table S2. Variance table for NG cytocompatibility (%)

Source	Sum of Squares	df	Mean Square	F-value	p-value	
Model	9005.82	5	1801.16	85.03	< 0.0001	significant
A-Mr	7438.61	1	7438.61	351.16	< 0.0001	***
A^2	1262.35	1	1262.35	59.59	< 0.0001	***
B^2	359.23	1	359.23	16.96	0.0005	***
A^2B	110.35	1	110.35	5.21	0.0330	*
A^2B^2	497.34	1	497.34	23.48	< 0.0001	***
Residual	444.85	21	21.18			
Lack of Fit	45.11	3	15.04	0.6771	0.5773	not significant
Pure Error	399.74	18	22.21			
Cor Total	9450.67	26				

Table S3. Coefficients table for NG cytocompatibility (%)

Factor	Coefficient Estimate	df	Standard Error	95% CI Low	95% CI High	VIF
Intercept	106.87	1	3.00	100.64	113.11	
A-Mr	-20.33	1	1.08	-22.58	-18.07	1.00
A^2	-28.61	1	3.71	-36.32	-20.90	3.89
B^2	-15.08	1	3.66	-22.69	-7.46	3.00
A^2B	-3.03	1	1.33	-5.80	-0.26	1.04
A^2B^2	21.86	1	4.51	12.48	31.24	5.89

Table S4. Variance table for NG size (nm)

Source	Sum of Squares	df	Mean Square	F-value	p-value	
Model	2.081E+05	8	26015.04	62.86	< 0.0001	significant
A-Mr	25963.65	1	25963.65	62.74	< 0.0001	***
B-Qd/Qc	35898.14	1	35898.14	86.74	< 0.0001	***
AB	1792.67	1	1792.67	4.33	0.0538	.
A^2	3417.99	1	3417.99	8.26	0.0110	*
B^2	204.60	1	204.60	0.4944	0.4921	
A^2B	2548.06	1	2548.06	6.16	0.0246	*
AB^2	15246.08	1	15246.08	36.84	< 0.0001	***
A^2B^2	9197.32	1	9197.32	22.22	0.0002	***
Pure Error	6621.75	16	413.86			
Cor Total	2.147E+05	24				

Table S5. Coefficients table for NG size (nm)

Factor	Coefficient Estimate	df	Standard Error	95% CI Low	95% CI High	VIF

Intercept	273.44	1	13.62	244.57	302.30	
A-Mr	-92.48	1	11.68	-117.24	-67.73	5.27
B-Qd/Qc	77.35	1	8.31	59.74	94.96	3.09
AB	-12.22	1	5.87	-24.67	0.22	1.04
A^2	51.55	1	17.94	13.52	89.57	4.48
B^2	-11.59	1	16.48	-46.52	23.35	2.61
A^2B	25.24	1	10.17	3.68	46.80	3.09
AB^2	81.31	1	13.40	52.91	109.70	5.22
A^2B^2	-100.12	1	21.24	-145.14	-55.10	6.38

Table S6. Variance table for NG PDI (-)

Source	**Sum of Squares**	**df**	**Mean Square**	**F-value**	**p-value**	
Model	0.0213	4	0.0053	21.27	< 0.0001	significant
A-Mr	0.0020	1	0.0020	8.08	0.0101	*
B-Qd/Qc	0.0161	1	0.0161	64.38	< 0.0001	***
AB	0.0016	1	0.0016	6.52	0.0189	*
B^2	0.0031	1	0.0031	12.26	0.0022	**
Residual	0.0050	20	0.0002			
Lack of Fit	0.0016	4	0.0004	1.85	0.1692	not significant
Pure Error	0.0034	16	0.0002			
Cor Total	0.0263	24				

Table S7. Coefficients table for NG PDI (-)

Factor	**Coefficient Estimate**	**df**	**Standard Error**	**95% CI Low**	**95% CI High**	**VIF**
Intercept	0.0150	1	0.0069	0.0007	0.0294	
A-Mr	-0.0113	1	0.0040	-0.0196	-0.0030	1.01
B-Qd/Qc	-0.0299	1	0.0037	-0.0377	-0.0221	1.03
AB	0.0115	1	0.0045	0.0021	0.0209	1.01
B^2	0.0282	1	0.0080	0.0114	0.0449	1.03

Table S8. Variance table for χ_{LPEI} (-)

Source	**Sum of Squares**	**df**	**Mean Square**	**F-value**	**p-value**	
Model	0.0211	2	0.0105	36.19	0.0004	significant
A-Mr	0.0192	1	0.0192	65.96	0.0002	***
A^2	0.0019	1	0.0019	6.42	0.0444	*
Residual	0.0017	6	0.0003			
Cor Total	0.0228	8				

Table S9. Coefficients table for χ_{LPEI} (-)

Factor	**Coefficient Estimate**	**df**	**Standard Error**	**95% CI Low**	**95% CI High**	**VIF**
Intercept	0.8266	1	0.0099	0.8025	0.8507	
A-Mr	0.0566	1	0.0070	0.0395	0.0736	1.00
A^2	-0.0306	1	0.0121	-0.0601	-0.0011	1.00

Table S10. Variance table for M∞ (%)

Source	Sum of Squares	df	Mean Square	F-value	p-value	
Model	0.0002	5	0.0000	34.91	< 0.0001	significant
A-Mr	0.0000	1	0.0000	32.70	< 0.0001	***
B-Qd/Qc	0.0000	1	0.0000	38.82	< 0.0001	***
A^2B	0.0001	1	0.0001	67.27	< 0.0001	***
AB^2	0.0000	1	0.0000	18.31	0.0004	***
A^2B^2	0.0001	1	0.0001	74.63	< 0.0001	***
Residual	0.0000	20	1.247E-06			
Lack of Fit	4.998E-06	3	1.666E-06	1.42	0.2716	not significant
Pure Error	0.0000	17	1.173E-06			
Cor Total	0.0002	25				

Table S11. Coefficients table for M∞ (%)

Factor	Coefficient Estimate	df	Standard Error	95% CI Low	95% CI High	VIF
Intercept	0.0181	1	0.0003	0.0175	0.0188	
A-Mr	-0.0029	1	0.0005	-0.0040	-0.0019	3.60
B-Qd/Qc	-0.0028	1	0.0004	-0.0037	-0.0019	2.85
A^2B	0.0045	1	0.0006	0.0034	0.0057	2.85
AB^2	0.0027	1	0.0006	0.0014	0.0041	3.62
A^2B^2	-0.0041	1	0.0005	-0.0050	-0.0031	1.04

Table S12. Variance table for cellular uptake (a.u.)

Source	Sum of Squares	df	Mean Square	F-value	p-value	
Model	22.11	6	3.68	252.57	< 0.0001	significant
A-Mr	12.79	1	12.79	876.33	< 0.0001	***
AB	0.2721	1	0.2721	18.65	0.0003	***
A^2	4.86	1	4.86	332.85	< 0.0001	***
B^2	1.09	1	1.09	74.57	< 0.0001	***
AB^2	5.66	1	5.66	388.21	< 0.0001	***
A^2B^2	2.84	1	2.84	194.49	< 0.0001	***
Residual	0.2918	20	0.0146			
Lack of Fit	0.0034	2	0.0017	0.1051	0.9008	not significant
Pure Error	0.2884	18	0.0160			
Cor Total	22.40	26				

Table S13. Coefficients table for cellular uptake (%)

Factor	Coefficient Estimate	df	Standard Error	95% CI Low	95% CI High	VIF
Intercept	2.21	1	0.0787	2.04	2.37	
A-Mr	-1.69	1	0.0572	-1.81	-1.57	4.03
AB	0.1506	1	0.0349	0.0779	0.22	1.06
A^2	1.76	1	0.0964	1.56	1.96	3.82
B^2	0.8298	1	0.0961	0.6293	1.03	3.00
AB^2	1.36	1	0.0692	1.22	1.51	3.96
A^2B^2	-1.64	1	0.1177	-1.89	-1.40	5.82

Table S14. Variance table for NE (%)

Source	Sum of Squares	df	Mean Square	F-value	p-value	
Model	85217.56	5	17043.51	69.03	< 0.0001	significant
A-Mr	2355.43	1	2355.43	9.54	0.0056	**
B-Qd/Qc	16280.01	1	16280.01	65.93	< 0.0001	***
AB	3340.47	1	3340.47	13.53	0.0014	**
A^2	337.93	1	337.93	1.37	0.2552	
A^2B	1549.78	1	1549.78	6.28	0.0205	*
Residual	5185.18	21	246.91			
Lack of Fit	1884.92	3	628.31	3.43	0.0394	significant
Pure Error	3300.26	18	183.35			
Cor Total	90402.74	26				

Table S15. Coefficients table for NE (%)

Factor	Coefficient Estimate	df	Standard Error	95% CI Low	95% CI High	VIF
Intercept	106.85	1	5.28	95.86	117.84	
A-Mr	-11.54	1	3.74	-19.31	-3.77	1.02
B-Qd/Qc	-51.15	1	6.30	-64.25	-38.05	3.00
AB	16.38	1	4.45	7.12	25.65	1.02
A^2	7.57	1	6.47	-5.89	21.03	1.02
A^2B	-19.33	1	7.72	-35.37	-3.28	3.02